C-7-3
Extended Abstracts of the 2004 International Conference on Solid State Devices and Materials, Tokyo, 2004, pp. 776-777

Study of Mobility in Strained Silicon and Germanium Ultra Thin Body MOSFETs

Tony Low [1,3], Chen Shen [1], M. F. Li [1,2], Yee-Chia Yeo [1], Y. T. Hou [1,2], Chunxiang Zhu[1], Albert Chin[4], L. Chan [3], D. L. Kwong [5]
(1) Silicon Nano Device Lab (SNDL), ECE Department, National University of Singapore, Singapore 119260. Email: elelimf@nus.edu.sg
(2)Institute of Microelectronis, Singapore, 117685; (3) Technology Development, Chartered Semiconductor Manufacturing, Singapore
(4) Dept Electronics Eng., National Chiao Tung Univ., Taiwan; (5) Dept. Electrical and Computer Engineering, University of Texas, Austin, TX 78712, USA

1. Introduction

Electron mobility in strained Si and Ge ultrathin-body (UTB) MOSFETs with sub-10 nm body thickness T_{body} is studied in this paper. In the literatures, only little is known about the carrier mobility in such devices [1-3] despite the fact that low longitudinal field mobility is still important [4,5]. In this paper, an accurate and calibrated physical model that takes the effect of scattering due to optical phonons, acoustic phonons, surface roughness, and interface states into account is used. We found that biaxial tensile strained-Si offers mobility enhancement down to $T_{body} \cong$ 3nm, below which quantum confinement effect gives the same benefit as strain effects, rendering the application of strain to Si redundant. In Ge channel UTB transistors, electron mobility is found to be highly dependent on surface orientation. Ge<100> and Ge<110> surface have low quantization mass that leads to high susceptibility to surface roughness, resulting in even lower mobility than Si in aggressively scaled UTB. Ge<111> with its higher quantization mass and low density of states mass is highly advantageous to channel mobility for aggressively scaled body.

2. Physical Model for Electron Mobility in UTB

Electronic structures for the two-dimensional electron gas are obtained by solving the coupled Schrödinger-Poisson equation self-consistently within the effective mass framework according to Stern [6]. Important bandstructure parameters such as conduction valleys energy minima and their ellipsoidal forms used are obtained from Fischetti [7] (Table 1). Transport masses in the device coordinate are derived by employing suitable unitary transformation [6, 8], such as to preserve the density-of-states mass in our context of low longitudinal field. The scattering matrix elements due to acoustic phonons (AP), optical phonons (OP), surface roughness (SR) and interface states (DIT) related scattering are formulated (Fig 10, 11 caption). The scattering rate is obtained by Fermi Golden Rule. We obtained the numerical solutions of the scattering time to the Boltzmann equation in Ohmic regime by embracing the relaxation time approximation under detailed balance condition [18, 19].

3. Experimental Results and UTB Mobility Modeling

Our physical model is calibrated using experimental Si mobility data [20], showing good agreement. An acoustic deformation potential of 15 eV [12, 18] was used. Using a deformation potential of 15 eV for intra-valley scattering within the L valleys of Ge, a mobility that is twice that of Si is obtained, in reasonable agreement with [21, 22]. A surface roughness autocorrelation function with root mean square Δ = 4Å and correlation length l =10Å is assumed for Si [23] and Ge [3] surfaces. A conservative interface states density of $1\text{x}10^{11}$ cm^{-2} for front and back interfaces is assumed. Our UTB device has a gate dielectric with an EOT of 1 nm, a metal gate electrode, and back oxide thickness of 50 nm. Fig 2 shows the calculated mobility for unstrained Si UTB transistor. It has been reported that as the Si body thickness is reduced [1, 24], mobility is reduced and deviates from the universal relationship. This was due to a variation in body thickness, i.e. δT_{Si}-induced scattering. This phenomenon can be captured via a body perturbation Hamiltonian H_{SR} (Fig 2), where V_P is a perturbed potential by a δT_{Si} of Δ_m, to be solved self-consistently, Δ_m the root mean square value, $\Delta(\boldsymbol{r})$ is the function describing the interface profile, z and $\boldsymbol{r}$ define distance perpendicular and parallel to the dielectric/silicon interface respectively. In the limit of large body thickness, universal relationship with effective field is thus obtained (Fig 2). This, in essence, explains the deviation from the universal relationship as body thickness is reduced to the order of the surface roughness, corroborating with experimental trend [1, 24] (Fig 3).

4. Strained Silicon for Mobility Enhancement

We then examine the impact of biaxial tensile strain of 2% on the band structure and electron mobility in UTB MOSFETs. The limited mobilities due to AP, OP, SR, and DIT are calculated as a function of T_{body} (Fig 10). Strain generally leads to enhancement for the dominant AP and SR limited mobilities for effective vertical field of 0.1MV/cm (threshold condition) and 1MV/cm (strong inversion condition) down to T_{body} of 3 nm. As T_{body} is reduced, the strong body confinement lifts the energy of the Δ_4 valleys, leading to more carrier occupation in the high mobility Δ_2 valleys and reduced carrier occupation at the Δ_4 valleys (Fig. 5). This effect is similar to the effect of biaxial tensile strain. When T_{body} is reduced below 3 nm, quantum confinement achieves the same effect as the strain considered; leading to comparable total mobilities for both strained and unstrained Si. This is illustrated for T_{body} = 2 nm in Fig. 4. In addition, the peak mobility observed in unstrained Si due to the subband level modulation [1] is smoothened out with applied strain. The mobility enhancement for SR limited mobility is appreciable for effective field at 0.5MV/cm (moderate inversion condition) and 1MV/cm, for T_{body} down to 4 nm. Subsequent drastic decrease of mobility at thinner body is attributed to the deviation of the perturbation Hamiltonian from direct effective field dependence.

5. Germanium UTB MOSFETs

We had systematically explored the performance limits of Ge UTB MOSFETs [25] relating to its electrostatics, ballistic current and leakage current. Here, we examine the impact of various crystal orientations on the mobility of Ge UTB transistors. Fig 6 compares the total effective mobility of UTB devices with Ge and Si channel at T_{body} of 2nm. While electron mobility in bulk Ge is higher than that in bulk Si, Ge<110> and Ge<100> UTB devices have lower mobility than Si<100>. Ge<111> shows better mobility than Si<100> at T_{body} = 2 nm. We then evaluated the limited motilities of Ge<111> and Ge<110> to gain an understanding of the underlying physics. Fig 11 plots the various limited mobilities for Ge<111> and Ge<110> as a function of T_{body}. As T_{body} is reduced, the gradual increase in form factor (the subband wave function overlap integral) for Ge<110> leads to a lower mobility [19]. However, the larger quantization mass of Ge<111> causes the carrier to reside nearer to the channel surface and hence its form factor is less sensitive to the body confinement effect. In particular, the SR limited mobility of Ge<110> is severely degraded as T_{body} is scaled down. Fig 7 highlights the general trend that at high effective field, the effective mobility decreases with reduced quantization mass. A larger quantization mass provides more efficient potential screening, hence reducing the overall SR perturbation potential (Fig 7 inset). Fig 8 illustrates the perturbing potential felt at the same surface roughness condition for Ge<110> and Ge<111>. The small quantization mass of Ge<110> renders it very sensitive to the surface roughness condition, resulting in exponential increase of perturbing potential with reduction in T_{body} and subsequent mobility degradation (Fig 11). Electron mobility of various UTB transistors are summarized in Fig 9.

References: [1] K. Uchida, IEDM, p.47, 2002 [2] K. Rim, IEDM, p.49, 2003 [3] S. Nakaharai., APL**83**, p.3516, 2003 [4] M. S. Lunstrom, EDL**22**, p293, 2001 [5] M. S. Lundstrom, IEDM, p.789, 2003 [6] F. Stern, PR**163**, p.816, 1967 [7] M. V. Fischetti, JAP**80**, p2234, 1996 [8] A. Rahman, IEDM, p.471, 2003 [9] C. Jacoboni, RMP **55**, p.645, 1983 [10] C. Jacoboni, PRB **24**, p.1014, 1981 [11] P. J. Price, Ann. Phys **133**, p.217, 1981 [12] C. Jungemann, SSE**36**, p.1529, 1993 [13] M. V. Fischetti, PRB**48**, p.2244, 1993 [14] F. Gamiz, JAP**86**, p.6854, 1999 [15] Y. C. Cheng, Surf. Sci. **27**, p.663, 1971 [16] T. Ando, J. Phys. Soc. Jpn**43**, p.1616, 1977 [17] J. Lee, JAP**54**, p.6989, 1983 [18] D. Esseni, TED**50**, p.1665, 2003 [19] D. Esseni, IEDM, p.719, 2002 [20] S. Takagi, TED**41**, p.2357, 1994 [21] C. M. Ransom., TED**38**, p.2695, 1991 [22] C. H. Huang, IEDM, p.319, 2003 [23] T. Sugano, Surf. Sci**98**, p.154, 1980 [24] K. Uchida, IEDM, p.805, 2003 [25] T. Low, IEDM, p.691, 2003

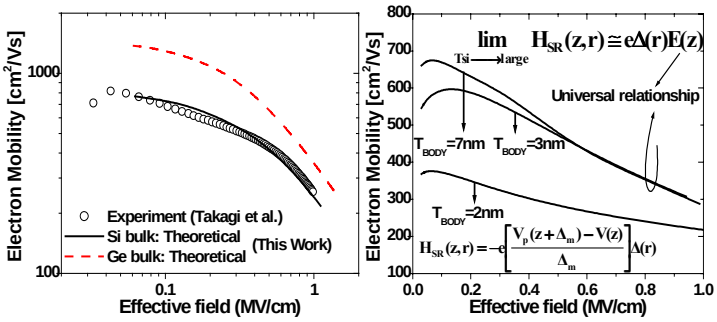

(L) Fig 1: Calibration of our theoretical low-field mobility model with experimental results for Si [15], showing excellent agreement. A two times mobility for Ge is obtained [21, 22] by fitting the technological dependent acoustic deformation potential for L valleys **(R) Fig 2:** Theoretical calculated total effective mobility curve for Si UTB at various body thicknesses demonstrating an explanation for the non-universality of mobility relationship with effective field (Fig 3). Effective field is the calculated mean electric field.

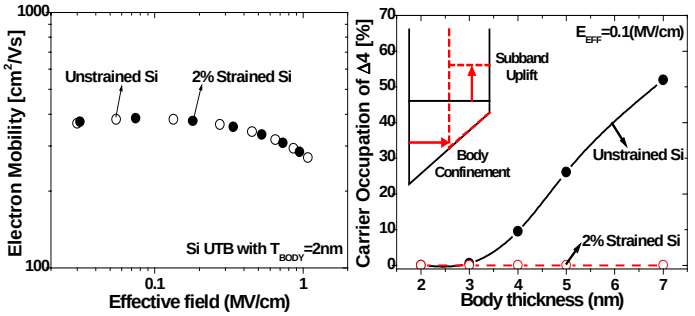

(L) Fig 4: Strong quantum confinement in aggressively scaled UTB (body thickness 2nm) renders the strained induced valley splitting using biaxial tensile strain (2%) redundant, leading to same low field mobility as unstrained device **(R) Fig 5:** Strong body confinement in unstrained Si results in subband energy uplift, reducing carrier occupation in Δ4 valley (with lighter mz, Table 1). At body thickness 3nm, Δ4 valley occupation is negligible, strain induced valley splitting will be redundant.

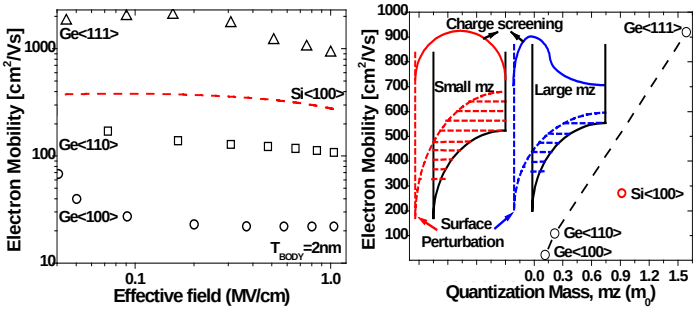

(L) Fig 6: High mobility in bulk Ge does not always translate to high mobility in Ge UTB transistor. Choice of surface orientation has a huge impact on device low field mobility. **(R) Fig 7:** High quantization mass mz, is critical for aggressively scaled UTB device. **Inset:** Energy band (along gate confinement) diagram illustrating effect of surface perturbation on small and large mz. A higher quantization mass propagates the electron nearer to the interface, providing more effective potential screening and reducing the overall perturbation potential. Simulated at body thickness 2nm and E_{EFF}=1MV/cm

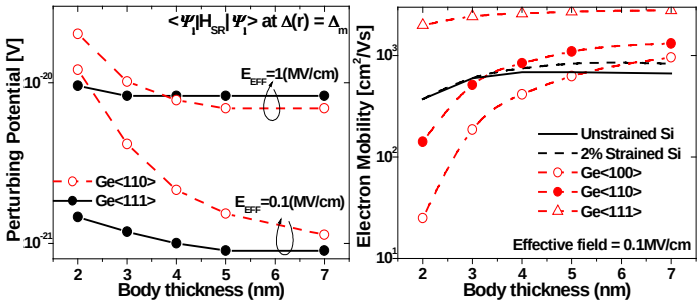

(L) Fig 8: Perturbation potential at $\Delta(r) = \Delta_m$ as function of body thickness for the lowest subband for a low mz (Ge<110>) and large mz (Ge<111>). Carriers experience larger perturbing potential as body is scaled down. Poorer charge screening for carriers with low mz render it very susceptible to surface roughness perturbation, aggravating at smaller body thickness. **(R) Fig 9:** Electron mobility for various advanced bandstructure UTB transistors as function of body thickness. Large mz and small md of Ge<111> (Table 1) provides the excellent high channel mobility.

Table 1: mz: quantization md: density of state mc: conductivity effective mass. Es: energy split (eV) ref. Ec of Si. g: degeneracy. (*): strain 2%

	valley	mz	md	mc	Es	g
Si<100>	Δ2	0.916	0.190	0.190	0 (-0.17)*	2
	Δ4	0.190	0.417	0.315	0 (+0.37)*	4
Ge<100>	L	0.117	0.295	0.149	0	4
	Δ	0.950	0.200	0.200	0.15	2
Ge<110>	L	0.218	0.216	0.140	0	2
	L	0.080	0.357	0.316	0	2
Ge<111>	L	1.590	0.080	0.080	0	1

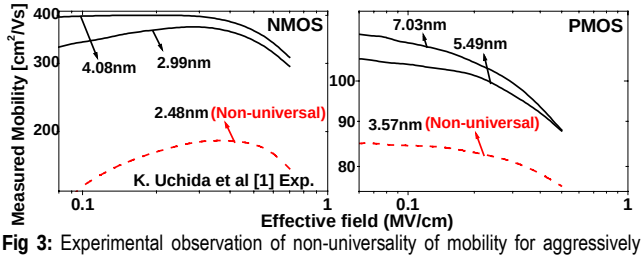

Fig 3: Experimental observation of non-universality of mobility for aggressively thin body [1] for both NMOS and PMOS. NMOS is more resistant to this phenomena, noticeable only at ~2.48nm whereas PMOS at ~3.57nm. This can also be consistently explained by our model as attributing to the smaller quantization mass of hole carriers (see Fig 7).

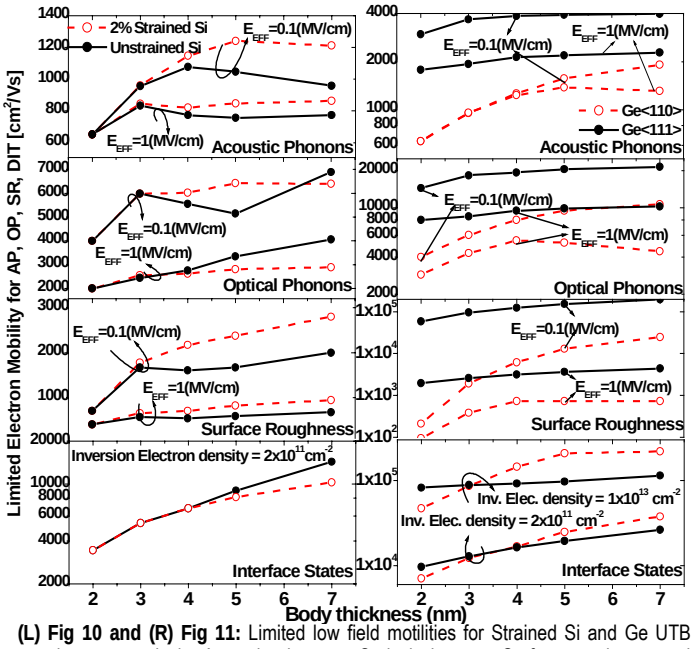

(L) Fig 10 and (R) Fig 11: Limited low field motilities for Strained Si and Ge UTB transistor respectively. Acoustic phonons, Optical phonons, Surface roughness and Interface charge limited mobilities are all systematically explored. All limited mobilities are plotted at constant effective field of 0.1MV/cm (threshold condition) and 1MV/cm (high inversion condition) except for interface charge limited mobility plotted at constant electron density criterion. **Formulation of scattering matrix elements:** Model for phonon spectrum in the bulk semiconductors are adapted from Jacobini et al [9, 10] where the matrix elements of the electron-phonon interaction are considered in a conventional way in accordance with Price [11, 12, 9]. Intra-valley acoustic phonon (AP) with an effective isotropic deformation potential [9, 12], intra-valley optical phonon (OP) for L valleys [9, 10] and inter-valley phonons constraint within the selection rules for f and g type processes [9] are accounted for. Dynamic screening of phonons is also disregarded [13]. Surface roughness (SR) scattering is treated in similar spirit as Gamiz et al [14] by extending Cheng's original treatment [15, 16] to account for the inefficacy of the linear expansion of the perturbed potential. The autocorrelation function of the asperities is assumed to be Gaussian. The static dielectric function for quasi-two-dimensional electron gas, based on a time-dependent perturbation approach [17] is employed for the treatment of screening [12]. Inter-subband transitions are left unscreened and the dielectric matrix is expressed according to [12] and in the quantum size limit when applicable. Interface states (DIT) induced scattering potential according to Stern et al [6] based on a perturbative approach is employed. By imposing appropriate boundary conditions, the scattering potential in all region of interest can be obtained using Nystrom Method [18].

Acknowledgements: This work is supported by Singapore A*STAR R263-000-267-305 grant. We gratefully acknowledge the useful discussion with D. Esseni (DIEGM) on coulomb scattering. We appreciate the useful discussion with M. V. Fischetti (IBM Corporation) and D. K. Ferry (Arizona State University) pertaining to their published literatures. We also thank S. Takagi (Tokyo University) for providing the experimental data to his classic paper [20]. T. Low gratefully acknowledge the scholarships from Singapore Millennium Foundation and Chartered Semiconductor Manufacturing.